SCIRES it
SCIentific RESearch and Information Technology
Ricerca Scientifica e Tecnologie dell'Informazione
Vol 15, Issue 1 (2025), 33-46
e-ISSN 2239-4303, DOI 10.2423/i22394303v15n1p33

CASPUR-CIBER Publishing, http://www.sciresit.it

UAS, LIDAR, GEOSLAM FOR 3D SURVEY OF NATURAL AND CULTURAL HERITAGE

Maria Grazia Cianci, Stefano Botta*, Daniele Calisi*, Sara Colaceci*, Vittoria Ghio**, Andrea Gullotta***, Michela Schiaroli**

* Department of Architecture, Roma Tre University – Rome, Italy.
** Department of Architecture and Design, Sapienza University of Rome – Rome, Italy.
*** MG Servizi di Ingegneria – Rome, Italy.

Abstract

This study applies an integrated methodology combining UAS photogrammetry, LIDAR, and SLAM laser scanning for the 3D survey of the Grotta Oscura quarries in Rome. A topographic network with GNSS RTK was established to ensure accurate georeferencing and alignment of heterogeneous datasets. Aerial surveys using drones captured high-resolution imagery and dense point clouds, while SLAM-based scanning documented underground environments. Data processing included orthophoto generation, dense 3D modeling, and point cloud integration. Software like Reality Capture, Autodesk Recap Pro, and GIS tools supported the analysis. The approach enabled detailed morphological assessment and virtual site navigation. Complex spatial relationships were modeled despite environmental constraints. This workflow demonstrates an effective strategy for surveying inaccessible heritage sites.

Keywords

UAS, LiDAR, geoSLAM, survey, cultural heritage

1. *Introduction*

Survey methodologies for natural cultural heritage have evolved significantly in recent years thanks to the integration of advanced technologies, including remote sensing, photogrammetry, satellite navigation systems and remotely piloted systems.

Digital photogrammetry, supported by images acquired by UAS (Unmanned Aerial System), has revolutionized the survey of natural cultural heritage (Remondino & Rizzi 2010). Recent studies show that the use of UAVs allows obtaining high-resolution orthophotos and digital terrain models, with an accuracy in the order of centimeters. The integration of photogrammetry with LiDAR (Light Detection and Ranging) allows improving the density of the point cloud and obtaining more precise data even in densely vegetated areas (Colomina & Molina, 2014).

Drones have established themselves as indispensable tools in monitoring natural and archaeological heritage.

The use of UAS for cultural heritage surveying allows overcoming the limitations of terrestrial methods, reducing operational costs and improving spatial coverage (Achille et al., 2015; Barba et al., 2020; Picchio, Parrinello & Barba, 2022; Russo et al., 2022a).

A further development is represented by mobile mapping, which integrates GNSS and LiDAR to collect dynamic geospatial data, particularly useful in karst environments and caves (Adinolfi et al., 2016; Warchoł et al., 2023).
The simultaneous use of different technologies, such as LIDAR and photogrammetry, is found in large fields of urban and territorial environment, demonstrating the need for the integration of multi-source data managed via point cloud (Bakuła et al., 2022).

Some research has experimented with survey techniques of natural sites with caves, therefore characterized by the presence of external and hypogeal environments, demonstrating the efficiency of the tools for the evaluation of structural interactions between the outside and the inside (Beltramone et al., 2024). Widely discussed issues are unfavorable environmental conditions, inaccessible areas or dangerous zone that require specific data acquisition procedures (Elias et al., 2024). A specific field of research, moreover, concerns archaeological areas, characterized by the presence of anthropic and architectural components, elements belonging to

Fig. 1: Aerial photograph of the Grotta Oscura Quarries (Source: Google Maps, ©2025 Airbus, CNES / Airbus, Landsat / Copernicus, Maxar Technologies, Map data ©2025).

different historical periods, coexistence of artificial and natural elements that require adequate skills and resources (Remondino & Campana, 2014; Rodríguez-Bulnes et al., 2022).

2. Case study

The archaeological area of the quarries of Grotta Oscura is located along Via Tiberina, on the right side of the Tiber in Rome, on one of the volcanic plateaus which characterize the Roman area. From above, the area features expansive meadow fields upon the volcanic plateaus, interspersed with woodlands on the slope sides. A feeder ditch of the Tiber crosses the area from North to South, while a hillside road provides access from the Via Tiberina to the site. This portion of land has been involved since antiquity in extraction activities; indeed, the underground area is occupied by a complex network of quarries. These elements underline the high naturalistic and landscape values of the site (fig. 1).

The quarries of Grotta Oscura represents an emblematic example of historical, cultural, and natural heritage. These ancient stone extraction sites, dating back to Roman times, have been utilized for centuries as a primary source of building materials. They have been significantly contributing to the architecture and urban planning of Rome, whose monuments and architectures owe part of their existence to the availability of these quarries (Coarelli, 2007). From a historical perspective, the caves have preserved evidence of human activities which extend beyond the Roman era, including medieval and modern uses, making the site a significant resource for industrial archaeology and the adaptation of human settlements. During conflicts such as World War II, their strategic importance became evident; the quarries were used as shelters and hiding places by civilians and military forces, emphasizing even more their strategic role (figs. 2-3). The landscape of the quarries of Grotta Oscura is as fascinating as its history. The area is characterized by high ecological value, stimulated in its growth by the morphological features of the cave site itself, where the underground galleries create a distinct environment that fosters the growth of biodiversity. The geological significance of the quarries of Grotta Oscura is further amplified by the presence of layers of various rock formations, offering a unique opportunity to understand the geological dynamics of the region. The subterranean galleries create unique microenvironments contributing significantly to local biodiversity. These layers narrate stories of climate change, tectonic movements, and volcanic

Fig. 2: Photograph of the Grotta Oscura Quarries site (Source: authors' photograph).

Fig. 3: Photograph of the interior of the underground quarries (Source: authors' photograph).

Fig. 4: DJI Matrice 350 RTK equipped with a DJI Zenmuse L1 LiDAR payload and a DJI Zenmuse P1 photographic payload; E-100 RTK GNSS receiver by e-Survey; GeoSLAM Zeb Horizon (Source: authors' photograph).

activity which have shaped the region over geological eras. Geological formations within the quarries offer insights into regional geological history, reflecting events such as climate change, tectonic shifts, and volcanic activities. The richness of this site provides research traces for geologists and climatologists, landscape architects, botanists, architects, historians, and anthropologists.

3. Data acquisition

The research group, coordinated by Maria Grazia Cianci from the Department of Architecture at Rome Tre University, in collaboration with MG Servizi di Ingegneria, focused on surveying the area of the quarries of Grotta Oscura in Rome through the integration of various techniques and remote sensing technologies (Cowley, 2014). This project integrates multiple advanced survey technologies and methodologies (figs. 4-5), selected specifically to address the site's unique morphological and environmental challenges. The survey of Grotta Oscura is highly complex due to specific environmental and operational conditions: extremely dense vegetation which make certain areas inaccessible; a very expansive site (90 hectares); hazardous areas which are difficult to access; a lack of a sufficiently high number of "visible" connections between underground zones and the exterior.

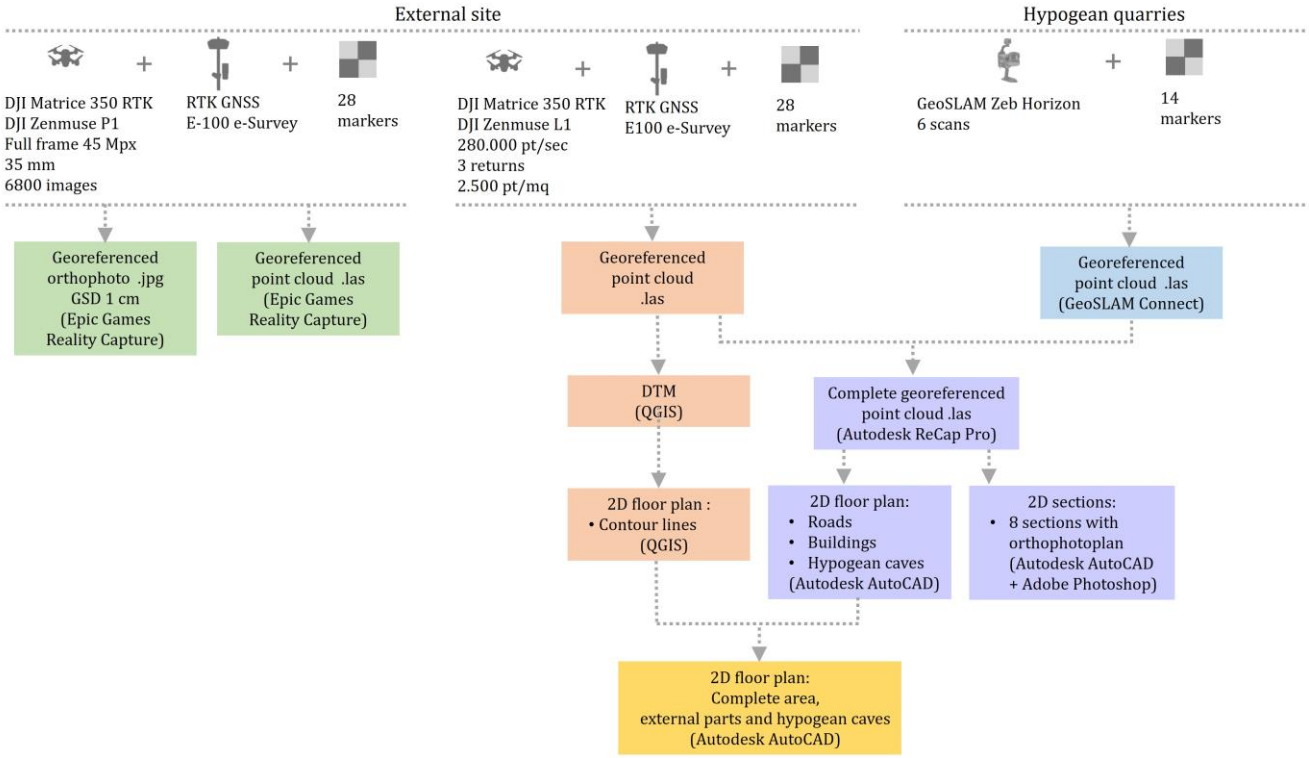

Fig. 5: Workflow (Source: author's graphical elaboration).

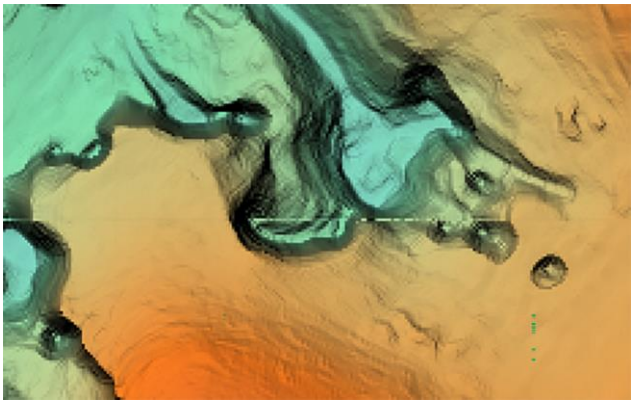

Fig. 6: Detail of top-view point cloud obtained from drone-based LiDAR acquisition: DTM (Source: authors' graphical elaboration).

For these reasons, various surveying techniques and methodologies were employed to ensure sufficient data coverage for conducting the analysis, understanding, and processing of the geometric and morphological data of the site, necessary for future recovery actions. The techniques and methodologies used are: a topographic network for anchoring the surveys and georeferencing the data; aerial photogrammetry via Unmanned Aircraft System (drones); aerial LIDAR scanning using Unmanned Aircraft System (drones); laser scanning with SLAM technology in underground areas (Remondino & Campana, 2014; Beltramone et al., 2024).

3.1 Topographic survey

A topographic network was established for the anchoring and integration of the surveys. The operation exploited also a E-100 RTK GNSS receiver from e-Survey, which is a multi-constellation, multi-frequency receiver capable of acquiring signals from 800 channels across the GPS, BDS, GLONASS, GALILEO, QZSS, and SBAS constellations (Scaioni, 2015).

The design of the topographic control network addressed a dual objective: on one hand, to ensure accurate georeferencing of the acquired data; on the other, to provide a coherent framework for registering heterogeneous datasets obtained through different survey techniques, specifically UAS-based LiDAR and SLAM-based laser scanning, within a complex area characterized by the presence of underground quarries.

The geomorphological and environmental conditions of the study area imposed significant

Fig. 7: Aerial photograph with 28 ground markers. In orange, non-accessible points. (Source: authors' graphical elaboration).

constraints on the design of the network. The combination of dense vegetation cover and widespread surface collapse features (fig. 11) makes direct and safe access to the subsurface particularly challenging. In this preliminary phase—aimed at producing a qualitative representation of instability conditions and fracture patterns within the quarries—minimizing the time spent inside the cavities was considered

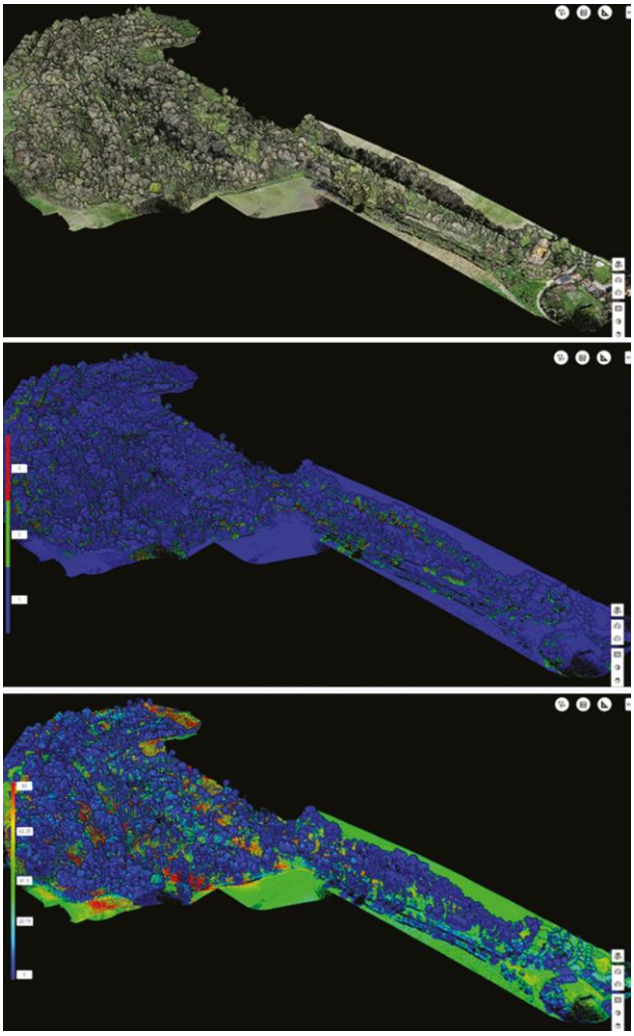

Fig. 8: Point cloud obtained from drone-based LiDAR acquisition: (a) RGB; (b) reflectance; (c) three returns; (d) (Source: authors' graphical elaboration).

essential. As a result, the use of traditional instruments such as total stations was ruled out.

To assess potential hazards beneath the vegetation, an initial UAS-based LiDAR survey was conducted. Although not georeferenced, this dataset was useful for detecting morphological anomalies indicative of subsurface instability (fig. 6). Simultaneously, the issue of metric connection between the interior and exterior of the cave system was addressed. The area has only four physical access points, of which only one is safely reachable. For the remaining three, an indirect solution was adopted: three topographic targets were placed via drone from outside the cave and are marked in orange in Fig. 6. These targets were strategically positioned to be visible not only from the outside via UAS imagery but also from within the cave using the SLAM laser scanner, despite being physically inaccessible.

The geographic coordinates of these targets were determined through photogrammetric processing and subsequently used to constrain the SLAM point cloud. Due to the site's constraints and the nature of the data, traditional point cloud registration techniques—such as cloud-to-cloud alignment and accuracy checks—could not be applied. The SLAM point cloud was rigidly anchored to the four known points, providing the only feasible solution for spatial integration at this stage. While this approach does not offer the highest level of accuracy, it is fully acceptable for the current qualitative phase of investigation and compatible with the survey's objective of assessing the state of fracturing within the quarry. Following structural stability assessments, more robust and accurate anchoring and registration strategies can be implemented. To support the photogrammetric reconstruction process, an additional 25 ground control points were distributed throughout the survey area. These targets were measured using GNSS RTK technology (E-100 antenna), carefully placed to ensure visibility in the UAS imagery and to provide a reliable basis for external alignment and metric calibration of the photogrammetric 3D model. A total of 28 ground points were determined over the area, indicated with topographic markers visible even from the drone. This approach allowed to establish a precise coordinate system, improving the integration of data coming from the different technologies used (fig. 7).

3.2 Aerial photogrammetric and LIDAR survey

An integrated aerial photogrammetric and LIDAR survey was conducted across the entire area of interest using drones. The drone employed was a DJI Matrice 350, equipped with an RTK Module, with an Operational Takeoff Mass of 7.2 kg, differential positioning systems, and collision-avoidance sensors LIDAR (Colomina & Molina, 2014; Nex & Remondino, 2014).

For the aerial photogrammetry, a DJI Zenmuse P1 photographic payload was used, featuring a 45MPx Full Frame sensor with a pixel size of 4.4 micrometers and a 35mm lens. The survey involved programmed flights capturing nadiral and oblique images at a 30° angle across the four cardinal directions: North, South, East, and West. A total of 6,800 high-resolution images were acquired. The aerial photogrammetric reconstruction process resulted in an average of 49,509 keypoints per image, with a mean internal

orientation reprojection error (RMS) of 0.47 pixels. The registration errors of the 25 external control points to the topographic network are reported in the table, with a maximum horizontal error of 5.47 mm and a maximum vertical error of 12 mm.

For the LIDAR survey, a DJI Zenmuse L1 LIDAR payload was employed, which includes a Livox

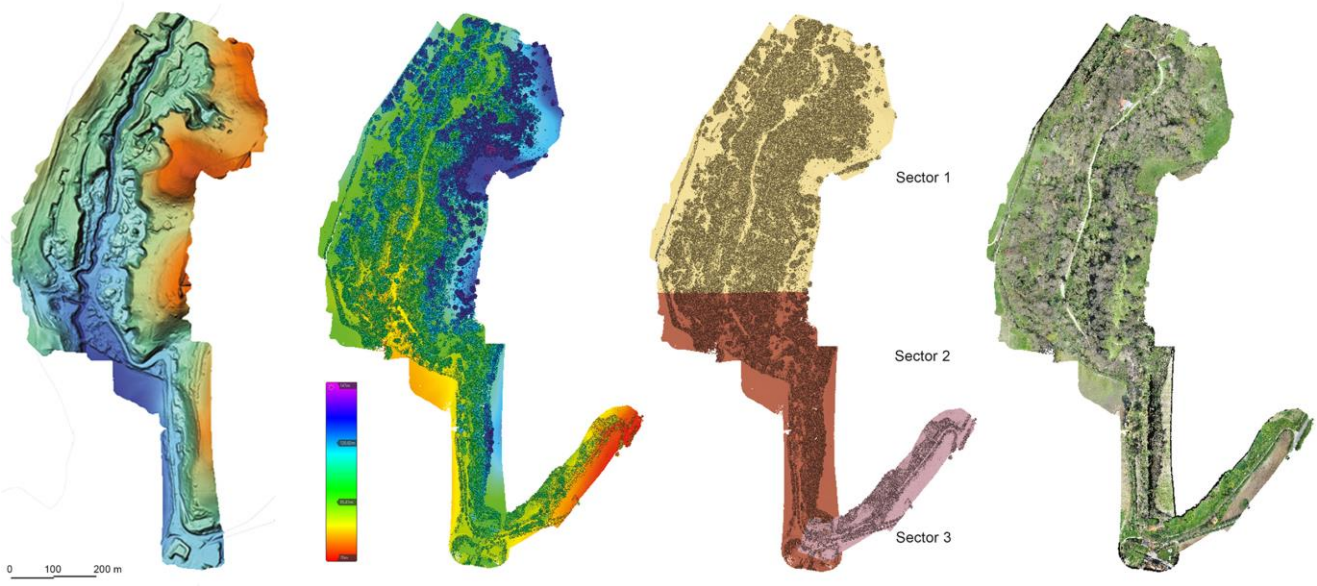

Fig. 9: Top-view point cloud obtained from drone-based LiDAR acquisition: DTM; point cloud visualized using the elevation function; three sectors; point cloud visualized in RGB (Source: authors' graphical elaboration).

Tab. 1: The registration errors of the 25 external control points to the topographic network.

Name	Category	RMS of Reprojection error [pixel]	3D Error [m]	Horizontal X Error [m]	Horizontal Y Error [m]	Vertical Error [m]
1	3D	0,7	0,011112	0,00387	0,004706	-0,009398
2	3D	0,65	0,012231	0,000858	0,001706	-0,013482
3	3D	0,68	0,009641	0,001464	0,001979	0,002776
4	3D	0,72	0,010004	0,00535	-0,000487	-0,003057
5	3D	0,63	0,012341	0,004608	0,000931	0,003944
6	3D	0,69	0,011907	0,00348	0,001358	0,012033
7	3D	7	0,013729	0,001898	0,004687	-0,009874
8	3D	0,68	0,010754	0,004388	-0,001597	-0,000931
9	3D	0,83	0,01085	0,003801	0,005381	0,004363
10	3D	0,72	0,013106	-0,000271	-0,002093	-0,009094
11	3D	0,75	0,014315	0,002632	0,005203	0,005566
12	3D	0,68	0,009984	0,002392	-0,001168	-0,012762
13	3D	0,75	0,012693	0,003023	0,002603	-0,00513
14	3D	0,79	0,012928	0,004307	0,000222	0,009985
15	3D	0,69	0,009582	-0,001371	0,001327	0,004726
16	3D	0,71	0,010333	0,005471	-0,000499	0,005268
17	3D	0,74	0,011947	-0,002115	-0,001281	-0,010686
18	3D	0,74	0,01407	-0,002444	-0,000995	0,001112
19	3D	0,78	0,011162	0,001968	0,001362	0,002245
20	3D	0,68	0,009679	-0,002504	-0,000269	-0,010905
21	3D	0,76	0,014082	-0,001836	0,000574	0,000841
22	3D	0,74	0,011475	-0,001918	-0,002981	-0,002015
23	3D	0,69	0,013712	7,70E-05	0,000851	0,004886
24	3D	0,72	0,013363	-0,003053	0,004107	0,002805
25	3D	0,76	0,012185	0,002893	-0,002114	-0,000409

Fig. 10: Point cloud obtained from drone-based LiDAR acquisition visualized in RGB.

Fig. 11: Photographic images acquired with DJI Matrice 350 RTK using the DJI Zenmuse P1 photographic payload (Source: authors' graphical elaboration).

LIDAR module, a high-precision IMU platform, and a 1-inch, 20MPx CMOS photographic sensor. The LIDAR module has a detection range of up to 450 meters, an effective point acquisition rate of 280,000 points/sec, and supports three returns with both repetitive and non-repetitive acquisition modes (figs. 8-9-10). The acquisitions were carried out with a ground point density of approximately 2,500 points/square meter. Reality Capture software from Epic Games was chosen for image processing and 3D reconstruction by photogrammetry (figs. 11-12-13).

Fig. 12: Orthophotomap generated from aerial photogrammetric processing (Source: authors' graphical elaboration).

Fig. 13: Point cloud obtained from aerial photogrammetric acquisition (Source: authors' graphical elaboration).

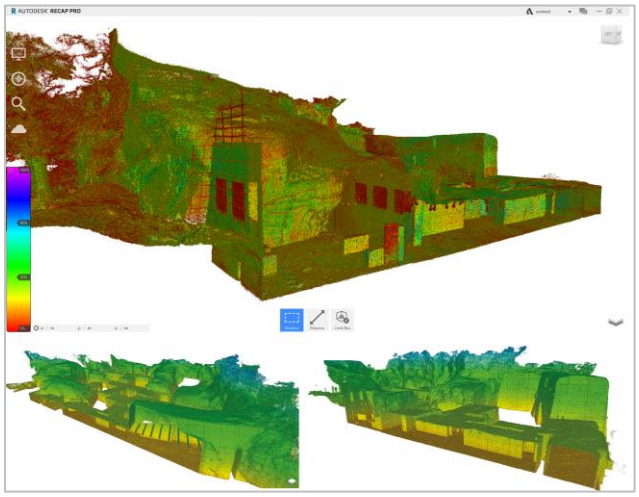

Fig. 14: Point cloud of the quarries acquired with GeoSLAM Zeb Horizon (Source: authors' graphical elaboration).

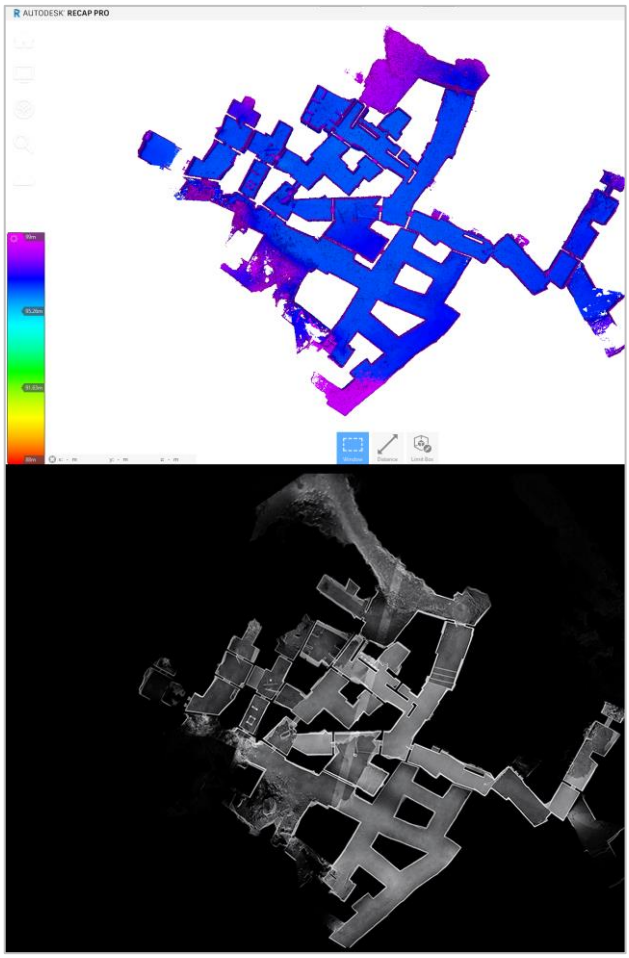

Fig. 15: Top-view point cloud of the quarries: visualized using the elevation function in Autodesk Recap Pro (top), visualized in PointCab (bottom) (Source: authors' graphical elaboration).

3.3 Laser scanning survey with SLAM technology

The complexity of the quarries did not allow the use of static laser scanners and photogrammetry. The interior of the caves was surveyed using mobile laser scanning technology with SLAM (Simultaneous Localization and Mapping) (Adinolfi et al., 2016; Warchoł et al., 2023).

The instrument used was a GeoSLAM Zeb Horizon, which has the following specifications: a range of 100 meters, a scanning speed of 300,000 points/sec, a relative accuracy of 6 mm, and 16 laser sensors. In total, six scans were performed, and 14 markers were placed for scan registration. Some of the markers were used for aligning the point cloud with the survey conducted externally by the drone (figs. 14-15).

This method has ensured the creation of high-density point clouds in complex environments that are difficult to detect with traditional techniques (Bakuła et al., 2022).

4. Data processing

The data processing phase required careful planning to ensure the smoothest and most consistent flow of information possible, given the variety of techniques and methodologies employed to survey both the surface portion and the underground section of the Grotta Oscura quarries.

4.1 Outputs from aerial photogrammetric process

The processing of data obtained from aerial photogrammetry involved the following steps: image cleaning, identification of topographic markers, aerotriangulation, and 3D model reconstruction. The results include: an orthophoto with a sampling distance of 1 cm in georeferenced JPG format; and a dense point cloud in LAS and E57 formats with point sampling at 2 cm (Luhmann et al., 2020). The orthophoto of the site provides the geometric configuration and texture visible from

Fig. 16: Quarry point cloud sections visualized in PointCab (Source: authors' graphical elaboration).

above, which is significant for dimensional analyses, identifying the alternation of vegetation components, and understanding landscape features. Despite some shadowed areas due to dense vegetation, the point cloud allows for virtual navigation of the site where physical access is impractical, and for making metric and morphological assessments.

4.2 Point cloud of the site

The point cloud of the area obtained from LIDAR was produced through a georeferenced dense point cloud (figs. 16). The LIDAR system employed supports three returns, allowing filtering of vegetation and the generation of both the DSM and the DTM (Elias et al., 2024). Thanks to georeferencing, the point cloud of the quarries (obtained through laser scanning with SLAM technology) was combined with the point cloud of the area (obtained from LIDAR) using Autodesk ReCap Pro. The digital navigation of the complete point cloud (both from the external area and the underground quarries) facilitated the site evaluation phase which was otherwise unfeasible on-site: exploring inaccessible areas due to dense vegetation, visualizing hazardous zones due to collapses, identifying areas at risk of collapse, controlling a very expansive area, and understanding the topographic relationship between the exterior and the underground environments (Ingman et al., 2020; Russo & Russo, 2022). Navigating the point cloud through elevation functions in Autodesk ReCap Pro allowed for an understanding of the morphological trends of the area, which consists of: a plateau reaching a maximum elevation (+130 m a.s.l.) extending from north to south and forming the main area where the caves have been excavated; a drainage ditch with its related areas reaching the lowest elevation (+81 m a.s.l.); and underground environments located at +96 m a.s.l.

4.3 Page CAD redrawing of the plan

As part of the investigation on the area, and in preparation for future preservation and recovery operations, it was necessary to draft a 2D layout of

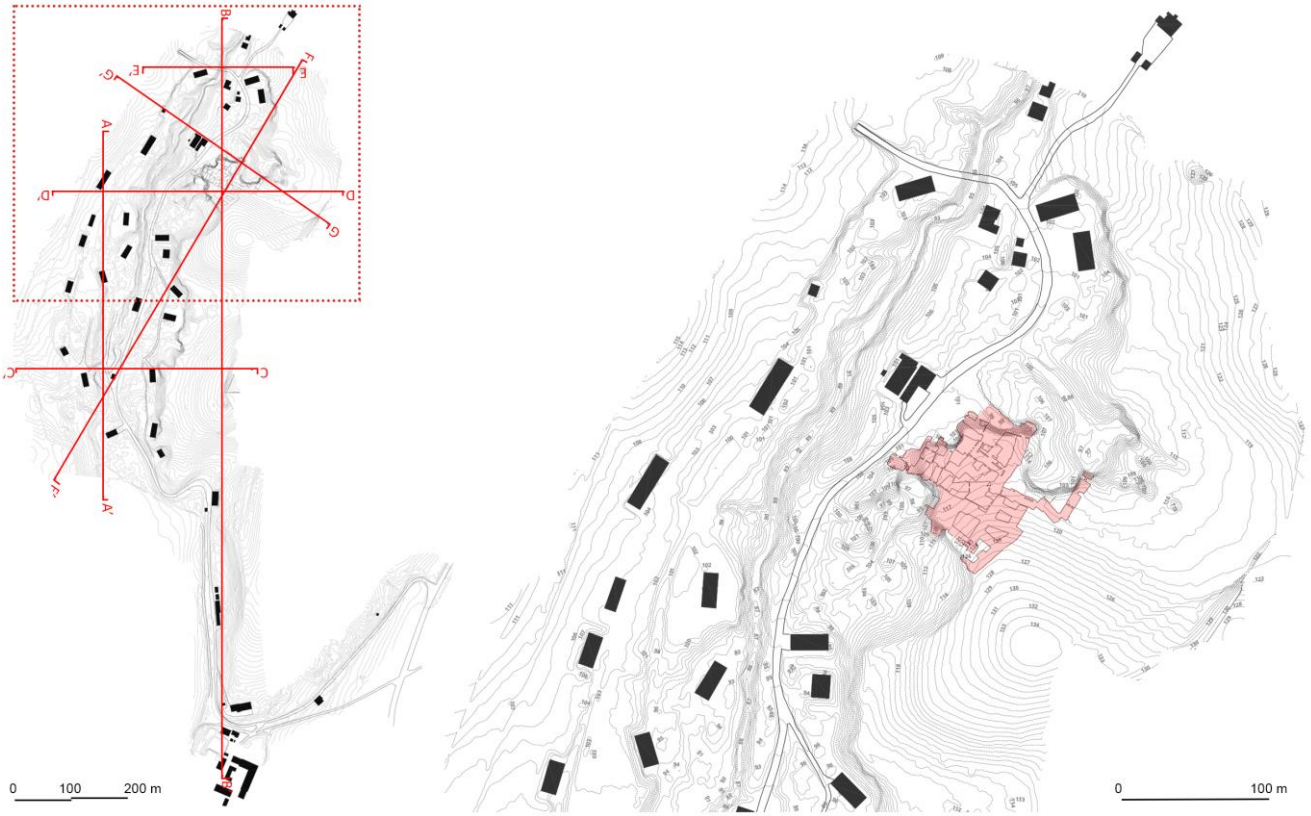

Fig. 17: CAD planimetric representation of the area (left); detail highlighting the quarries (right) (Source: authors' graphical elaboration).

the current state updated to 2024. The 2D plan was generated using various data sources: the point cloud from LIDAR processed in a CAD environment, and the DTM managed in a GIS environment. Initially, the DTM was imported into GIS (QGIS) to extract contour lines every meter. Subsequently, the complete point cloud (from both the external area and the underground quarries) was imported into CAD (Autodesk AutoCAD) to represent the internal passages layout of the site and its connection to the urban road Via Tiberina, as well as the abandoned buildings and underground environments. Finally, the contour lines extracted from the DTM were overlaid (Elias et al., 2024).

The vectorization of the site at a scale of 1:200 was essential to provide insight into the current state from spatial, geometric, and topographic perspectives, as well as the relationships between anthropogenic and natural components (fig. 17). The overlay of the vector 2D plan with the orthophoto obtained from aerial photogrammetry conveyed a planimetric visualization of the site enhanced with geometric and texture information (Rodríguez-Bulnes et al., 2022).

4.4 Orthophotos from LIDAR point cloud

The processing of eight orthophotos which cut across the site both transversely and longitudinally was necessary for multiple reasons: understanding the topographic trends across its territorial extent; comprehending the spatial and morphological relationships between external areas and underground environments; identifying the sequence of summit areas and lower zones; specifying vegetation masses along their altitudinal and planimetric extents (Remondino & Rizzi, 2010). The sectional orthophotos at a scale of 1:500 were obtained by importing the complete point cloud into CAD and setting up eight planes intersecting the point cloud. For each section, the following were extracted: the section line, the first plane including elements closest to the section plane, and the second plane including elements furthest from the section plane. Altimetric elevations above sea level were added for each section.

Beyond the geometric aspects, the work also focused on the visual representation of the orthophotos. Individual elements extracted in CAD

Fig. 18: Sections DD' and GG': orthophotomaps of the area obtained by integrating the LiDAR-based point cloud and the GeoSLAM point cloud, processed in CAD and Adobe Photoshop (Source: authors' graphical elaboration).

were exported as PDF and imported into a raster environment (Adobe Photoshop). Here, they were overlaid to manage the saturation and opacity of the first and second planes to impart greater spatial depth to the visual reading of each orthophoto (figs. 18).

2. *Conclusions*

The Grotta Oscura quarries have a rich historical, cultural, ecological, and geological heritage. Through the comprehensive integration of advanced survey methodologies, this research significantly contributes to the understanding, documentation, and preservation of Grotta Oscura's rich heritage. Such integrated approaches provide essential data and analytical resources to support strategic planning, conservation management, and sustainable enhancement of this historically and ecologically valuable landscape.

The mapping and specialized survey of these sites can facilitate the exploration of the connection between geodiversity and biodiversity, deepening the relation between the two fields. It also allows for the repositioning of geological assets, including quarries, which are often regarded as standalone objects, within a broader systemic and ecosystemic perspective.

In this context, the surveying work conducted allowed for the mapping and documentation of all the nuances and the richness of this location (Sobura et al., 2023; Adami et al., 2019; Colaceci et al. 2022; Federman et al. 2017). The investigation revealed the complexity of interactions between humans and nature within the quarries environment, underscoring the importance of preserving this geological and landscape heritage. These models are not only tools of representation but also resources for strategic planning, enabling the identification of areas most vulnerable to erosion and potential landslide risks. Furthermore, detailed documentation of the quarries is essential for promoting active conservation and sustainable management of this valuable heritage. This highlights the necessity of preserving the quarries of Grotta Oscura not only as silent testimonies of human history but also as vibrant ecosystems which deserve protection and enhancement for future generations.

REFERENCES

Achille C., Adami A., Chiarini S., Cremonesi S., Fassi F., Fregonese L., & Taffurelli L. (2015). UAV-based photogrammetry and integrated technologies for architectural applications - Methodological strategies for the after-quake survey of vertical structures in Mantua (Italy). *Sensors* 2015, *15*(7), 15520-15539. https://doi.org/10.3390/s150715520.

Adami, A., Fregonese, L., Gallo, M., Helder, J., Pepe, M., & Treccani, D. (2019). Ultra light UAV systems for the metrical documentation of Cultural Heritage: applications for architecture and archaeology. *International Archives of the Photogrammetry, Remote Sensing and Spatial Information Sciences - ISPRS Archives* (XLII-2/W17) 15–21. https://doi.org/10.5194/isprs-archives-XLII-2-W17-15-2019.

Adinolfi, O., Bonfanti, C., Mattioli, L., & Guardini, N. (2016). Strumenti e applicazioni con laser portatili I casi di FARO e GeoSLAM. *GEOmedia*, *19* (6). https://ojs.mediageo.it/index.php/GEOmedia/article/view/1282.

Bakuła, K., Lejzerowicz, A., Pilarska-Mazurek, M., Ostrowski, W., Górka, J., Biernat, P., Czernic, P., Załęgowski, K., Kleszczewska, K., Wężka, K., Gąsiewski, M., Dmowski, H., & Styś, N. (2022). Sensor integration and application of low-sized mobile mapping platform equipped with LIDAR, GPR and photogrammetric sensors. *International Archives of the Photogrammetry, Remote Sensing and Spatial Information Sciences - ISPRS Archives* (XLIII-B1-2022) 167–72. https://doi.org/10.5194/isprs-archives-XLIII-B1-2022-167-2022.

Barba, S., di Filippo, A. Ferreyra, C., & Limongiello, M. (2020). A pipeline for the integration of 3D data on aerophotogrammetric frameworks. The case study of Villa Rufolo. In S. Barba, S. Parrinello, M. Limongiello, A. Dell'Amico (Eds.). *D-SITE Drones - Systems of Information on culTural hEritage. For a spatial and social investigation* (pp. 32-39). Pavia: Pavia University Press.

Beltramone, L., De Lucia, V., Ermini, A., Innocenti, M., Silvestri, D., Rindinella, A., Ronchitelli, A., Ricci, S., Boschin, F., & Salvini, R. (2024). Applying SLAM-Based LiDAR and UAS Technologies to Evaluate the Rock Slope Stability of the Grotta Paglicci Paleolithic Site (Italy). *GeoHazards* 2024, 5, 457-484. https://doi.org/10.3390/geohazards5020024.

Bertolini, S., Piemonte, A., Caroti, G., Bevilacqua, M.G., Capriuoli, F., Rinaldi, E., Santillo, D., & Muccilli, I. (2024). Integrated 3D Survey Methodologies and Digital Platforms for the Enhancement of Archaeological Data in the Digital Transition. *SCIRES-IT - SCIentific RESearch and Information Technology, 14*(2), 107-124. http://dx.doi.org/10.2423/i22394303v14n2p107

Coarelli, F. (2007). *Rome and Environs: An Archaeological Guide*. Berkeley, Los Angeles:University of California Press.

Colaceci, S., Chiavoni, E., & Cianci, M.G. (2022). UAVs and GIS models for landscape representation. *DISEGNARECON 15* (29), 1-14. https://doi.org/10.20365/disegnarecon.29.2022.10.

Colomina, I., & Molina, P. (2014). Unmanned aerial systems for photogrammetry and remote sensing: A review. *ISPRS Journal of Photogrammetry and Remote Sensing*, *92*, 79-97. https://doi.org/10.1016/j.isprsjprs.2014.02.013.

Cowley, D.C. (ed.) (2010). Remote Sensing for Archeological Heritage Management. *11° EAC Heritage Management Symposium*, Reykjavik, Iceland, 25-27 March 2010.

Elias, M., Isfort, S., Eltner, A., & Maas, H.-G. (2024). UAS Photogrammetry for Precise Digital Elevation Models of Complex Topography: A Strategy Guide. *ISPRS Ann. Photogramm. Remote Sens. Spatial Inf. Sci.*, X-2-2024, 57–64. https://doi.org/10.5194/isprs-annals-X-2-2024-57-2024.

Federman, A., Santana Quintero, M., Kretz, S., Gregg, J., Lengies, M., Ouimet, C., & Laliberte, J. (2017). UAV photogrammetric workflows: a best practice guideline, *International Archives of the Photogrammetry, Remote Sensing and Spatial Information Sciences - ISPRS Archives* (XLII-2/W5), 237-244. https://doi.org/10.5194/isprs-archives-XLII-2-W5- 237-2017.

Ingman, M., Virtanen, J.-P., Vaaja, M.T., & Hyyppä, H. A (2020). Comparison of Low-Cost Sensor Systems in Automatic Cloud-Based Indoor 3D Modeling. *Remote Sens, 12* (2624), 1-20. https://doi.org/10.3390/rs12162624.

Luhmann, T., Robson, S., Kyle, S., & Boehm, J. (2020). *Close-range Photogrammetry and 3D Imaging*. Berlin, Boston: De Gruyter GmbH. https://doi.org/10.1515/9783110607253

Mediati, D., & Brandolino, R.G. (2024). Digital Surveying, Augmented Trekking and Valorisation Strategies for Inland Areas. The Grandi Pietre Valley. *SCIRES-IT - SCIentific RESearch and Information Technology, 14*(1), 79-96. http://dx.doi.org/10.2423/i22394303v14n1p79

Nex, F., & Remondino, F. (2014). UAV for 3D mapping applications: A review. *Applied Geomatics*, *6*(1), 1-15. Londra: Springer Nature. https://doi.org/10.1007/s12518-013-0120-x

Picchio, F, Parrinello, S. & Barba, S. (2022). Drones and Drawings - methods of data acquisition, management, and representation, *DISEGNARECON, 15* (29), 1-7. https://doi.org/10.20365/disegnarecon.29.2022.ed

Remondino, F., & Campana, S. (2014). *3D Recording and Modelling in Archaeology and Cultural Heritage: Theory and Best Practices*. Bicester: Archaeopress BAR.

Remondino, F., & Rizzi, A. (2010). Documentazione 3D basata sulla realtà di siti del patrimonio naturale e culturale: tecniche, problemi ed esempi. *Appl. Geomat.*, 2, 85–100.

Rodríguez-Bulnes, J., Benavides López, J.A., Romero Pellitero, P., Martín Civantos, J.M., & Rouco Collazo, J. (2022). The documentation of archaeological heritage through aerial photogrammetry and UAS-based LiDAR: the case study of the Espique valley (La Peza, Granada, Spain). *DISEGNARECON, 15* (29), 1-10. https://doi.org/10.20365/disegnarecon.29.2022.12.

Russo, M., Panarotto, F., Flenghi, G., Russo, V., & Pellegrinelli A. (2022a). Ultralight UAV for steep-hill archaeological 3D survey. *DISEGNARECON, 15* (29), 1-17. https://doi.org/10.20365/disegnarecon.29.2022.3.

Russo, M., & Russo, V. (2022b). Geometric analysis of a space grid structure by an integrated 3d survey approach. *Int. Arch. Photogramm. Remote Sens. Spatial Inf. Sci.*, XLVI-2/W1-2022, 465–472. https://doi.org/10.5194/isprs-archives-XLVI-2-W1-2022-465-2022.

Scaioni, M. (2015). *Modern Technologies for Landslide Monitoring and Prediction*. Berlin: Springer. https://doi.org/10.1007/978-3-662-45931-7.

Sobura, S., Bacharz, K., & Granek, G. (2023). Analysis of two-option integration of unmanned aerial vehicle and terrestrial laser scanning data for historical architecture inventory. *Geodesy and Cartography. 49* (2), 76–87. https://doi.org/10.3846/gac.2023.16990.

Warchoł, A., Karaś, T., & Antoń, M. (2023). Selected qualitative aspects of Lidar point clouds: GeoSLAM Zeb-Revo and Faro Focus 3D X130. *Int. Arch. Photogramm. Remote Sens. Spatial Inf. Sci.*, XLVIII-1/W3-2023, 205–212. https://doi.org/10.5194/isprs-archives-XLVIII-1-W3-2023-205-2023.